Mixing line parameterizations for cloudy boundary layers.

Alan K Betts
RR3, Box 3125, Pittsford, VT 05763

1. INTRODUCTION

It has been almost 25 years since I started work on the topic of cloudy boundary layers (CBL); so I thought I would attempt an overview of some basic issues in parametrizing CBL's. We are seeing at this workshop a wide range of approaches, which illustrate the importance and complexity of the topic. It is important, however, in GCM parametrization to frequently step back, and ask whether we have modelled the key processes in the simplest possible way, and whether these processes are interacting correctly. I hope this paper will serve as an introduction to this session.

My framework is this. From a modelling and observational perspective, the key issue for the CBL is (I believe) whether we can predict the correct equilibrium thermodynamic state (which I shall represent by potential temperature θ, and mixing ratio q) in situations over land and sea that are changing slowly; and the correct rates of change for CBL's forced from the surface; such as the diurnal cycle over land, or the advection of cold air over a warmer ocean. In this verbal definition, we immediately see the essential issue of timescale, so I shall first discuss the internal and external timescales (τ_I,τ_E) for the CBL. This separation is for conceptual convenience. The external or boundary timescales are those which determine the fluxes at the surface (surface wind, roughness, vegetation etc) and at CBL top (entrainment of air from above). The radiative process also has a comparable timescale to entrainment (*Betts*, 1989). The internal timescale is the timescale of mixing within the CBL. There may be different values for the cloud and subcloud layers. If $\tau_I << \tau_E$, then the CBL will have a nearly well-mixed structure, and correspondingly mixed layer models are useful simplifications. However even if a CBL is nearly well-mixed, its equilibrium state or time-change will not be correctly predicted in a model, if the boundary fluxes are wrong. Superficially the surface flux problem over the oceans is easier than over land (but still a problem at low wind speeds (eg *Miller et al*, 1992)). Over land, the surface fluxes during the daytime depend on the vegetation and soil moisture (and their time history) and the net radiation (which is controlled on a short time-scale by CBL cloud). The entrainment fluxes are not well-known, either for cloud-free BL's (*Betts et al* 1992), or for cloudy CBL's, which many papers here address. This is because entrainment is not really external at all. It is driven by the circulations within the BL, and may well differ significantly for circulations driven by surface fluxes, or radiative processes

interacting with the cloud layer.

But if we continue the conceptual separation of internal and external timescales a little longer, we can say that the ratio τ_I/τ_E controls how well-mixed a CBL is. This is important because it has a connection to cloud fraction. Well-mixed BL's over the ocean will generally always be capped with stratocumulus (*Betts*, 1989); while trade cumulus layers which have $\tau_I \sim \tau_E$ (and therefore are poorly mixed) have small cloud fractions. But since the clouds are the agent of mixing in CBL's, and their presence interacts with the radiation field to drive more mixing internally (as well as reducing surface net radiation over land); the coupling and feedback between the boundary fluxes, the internal structure and the cloud field is so tight, that it is not surprising that our attempts at parametrization have had limited success in GCM's.

I cannot solve this problem today, but I will take apart semi-quantitatively a few conceptual models and parametrizations to illustrate unsolved issues, and suggest a framework for assessing model schemes, whether in GCM's or those of much finer resolution. My approach to GCM parametrization has always been to look for the simplest representation of key processes; which in CBL's relate to the timescales of mixing and their interaction. The next section is a review distilled from some of my earlier papers on the use of conserved variable mixing diagrams in the study of the tradewind CBL.

2. TRADEWIND BOUNDARY LAYER EQUILIBRIUM

2.1 Tradewind cumulus on Mixing Diagrams

The conserved variable diagram I shall use is a plot of saturation potential temperature against saturation mixing ratio (*Betts*, 1982, 1985a, 1989). Fig 1 shows this diagram with superimposed lines of saturation pressure (solid) from 1000-600 mb. Shown are three important reference processes: the wet adiabat (solid) of $\theta_e^* = 350$ K, the wet virtual adiabat (dotted) of 350 K (which is the neutral stability line for cloud parcels rising adiabatically, including the density effects of liquid and water vapor), and the dry virtual adiabat of $\theta = 300$ K (which is the neutral stability line, including the density effect of water vapour in unsaturated parcels). The x axis is of course the dry adiabat of constant θ on this figure, and the y axis a line of constant q.

Fig 2 shows an example of the mean structure of a tradewind CBL in the E Equatorial Pacific from *Betts and Albrecht* (1987). (Consider Fig 2 superimposed on Fig 1.) The markers are saturation points for this mean

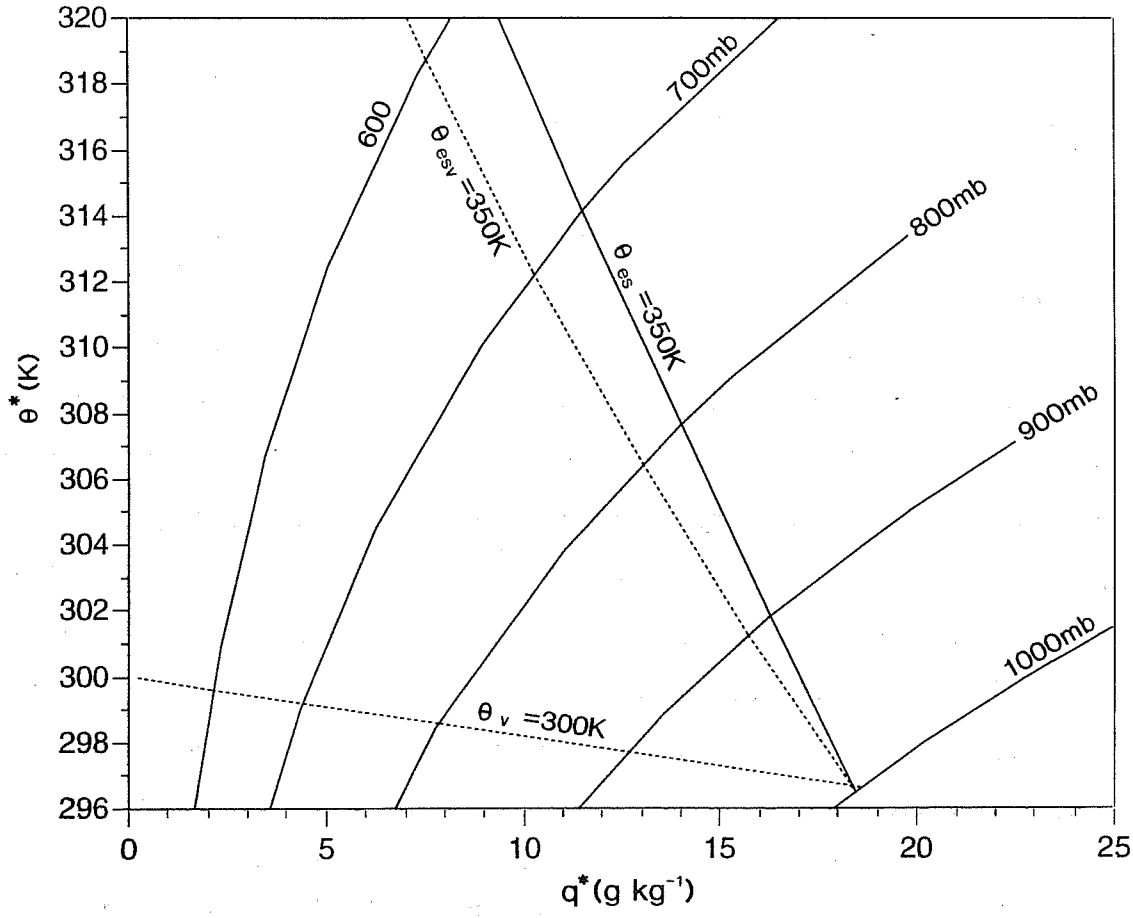

Fig. 1 **Conserved variable diagram (θ^*,q^*), showing constant saturation pressure lines, wet adiabat (solid), wet and dry virtual adiabats (dashed).**

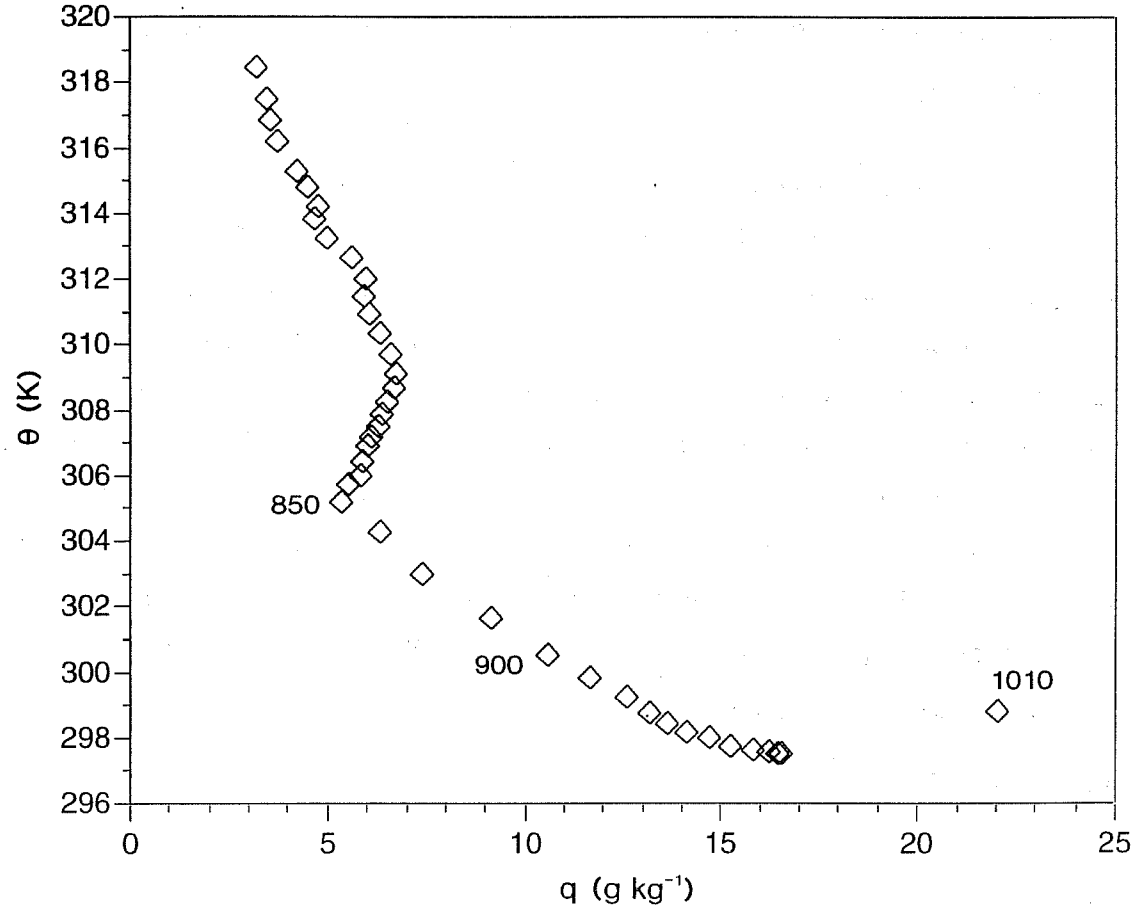

Fig. 2 **(θ,q) plot for E Equatorial Pacific average (#141) from *Betts and Albrecht* (1987).**

sounding at 10 mb levels, from saturation at the ocean surface pressure of 1010 mb on the far right to a pressure of 600 mb (with a saturation pressure p^* of 505 mb) on the far upper left. This is a characteristic thermodynamic distribution through an oceanic tradewind CBL. There is a weakly superadiabatic layer above the surface where θ falls $\approx$ 1.2 K, and q falls $\approx$ 5.5 gKg^{-1}: this appears as a jump in this data between the ocean surface data point at 1010 mb and the first atmospheric point at 1000 mb, which has a saturation level near 960 mb, corresponding to the tradewind cloud-base. There is a clustering of points near this saturation pressure, corresponding to air in the subcloud layer with $1000 > p > 970$ mb. This subcloud layer air is nearly well mixed; the timescale of mixing is quite fast ($\approx$1000 sec), because small perturbations in θ_v generate vertical velocities $\approx$ 1 ms^{-1} and its depth is only 500 m. Correspondingly, note that the distribution of SP from 1000 to 960 mb is parallel to a θ_v isopleth, the neutral density line. Above cloud-base, there is a smooth gradient of SP in the lower part of the trade-wind cumulus layer, which is less well mixed than the subcloud layer, and then a more rapid transition from say 900 to 850 mb which corresponds to the trade inversion. This partially mixed cumulus layer has a structure on this (θ,q) plot that is nearly linear, corresponding to a mixing line, with a slope between the dry and wet virtual adiabats. This is characteristic of partly cloudy CBL's. At 850 mb, the top of the inversion, the sounding has a sharp kink, where moisture increases with height at nearly constant $p^* \approx 670$ mb. This air has probably subsided (with radiative cooling) on timescales of order 5-6 days, after exiting a deep convective system near the freezing level in the mid-troposphere (*Betts and Albrecht*, 1987).

Now consider this CBL as an equilibrium between the surface fluxes, the entrainment fluxes and net radiative cooling. The subcloud layer equilibrium is a balance of four vectors (see *Betts*, 1984, 1992) shown schematically in Fig 3: a surface flux (driven by the surface wind) which moves this layer towards saturation at the ocean surface, a flux through cloud-base (the upward transport of moisture and downward transport of heat through cloud-base), radiative cooling, and a small vector for the effect of subsidence on this layer. At equilibrium, over 90% of the surface moisture flux is transported through cloud-base, and the surface and cloud-base heat fluxes together closely balance the radiative cooling (which is large for the moist subcloud layer over the tropical oceans ($\approx$-2.4 K day^{-1})). We can see that the subcloud layer is kept cooler than the ocean by this radiative cooling. The formal construction of this diagram can be summarized briefly as follows. The surface flux vector can be represented as a vector difference of SP's (saturation points) in terms of a bulk aerodynamic formula $gF_o = \omega_o \Delta S$ where

$$\Delta S = \Delta(C_p\theta, Lq) \tag{1}$$

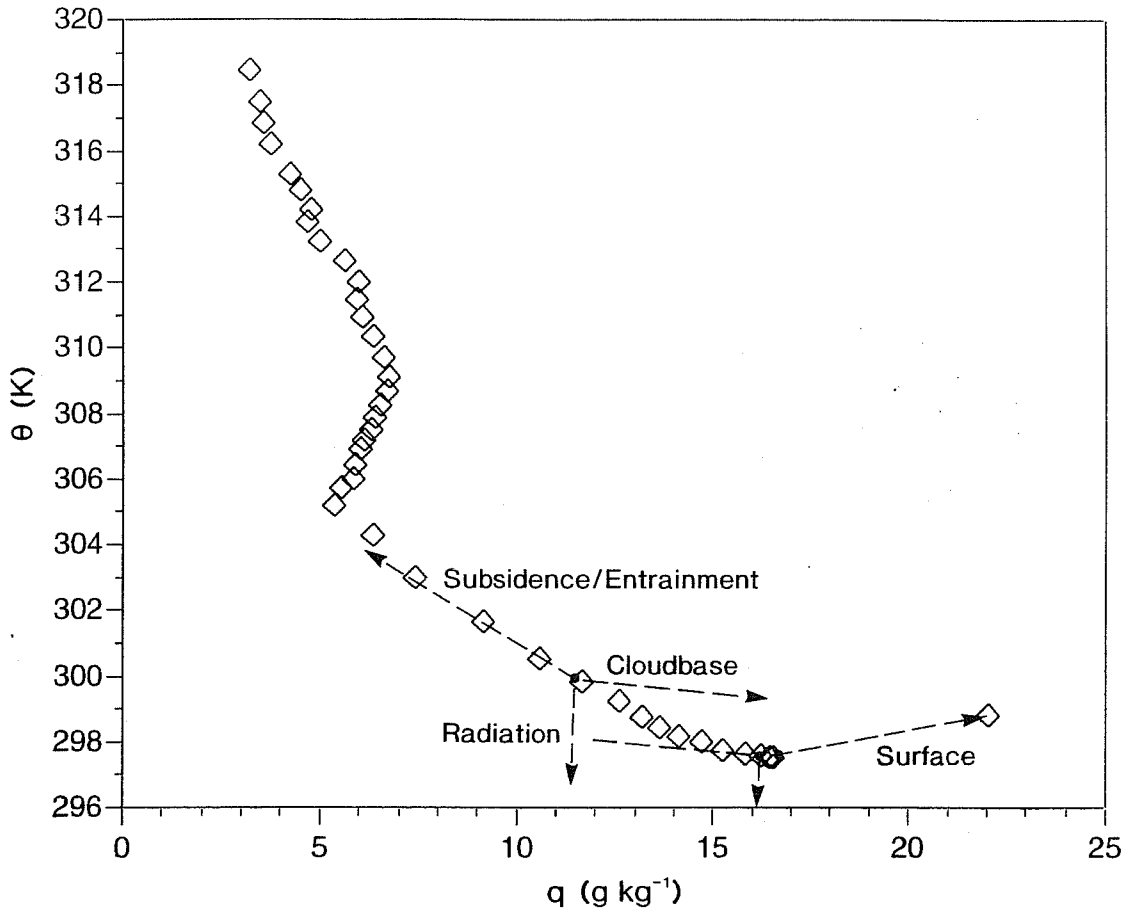

Fig. 3 As Fig 2 with schematic vector diagrams for thermodynamic balance of cloud and subcloud layers.

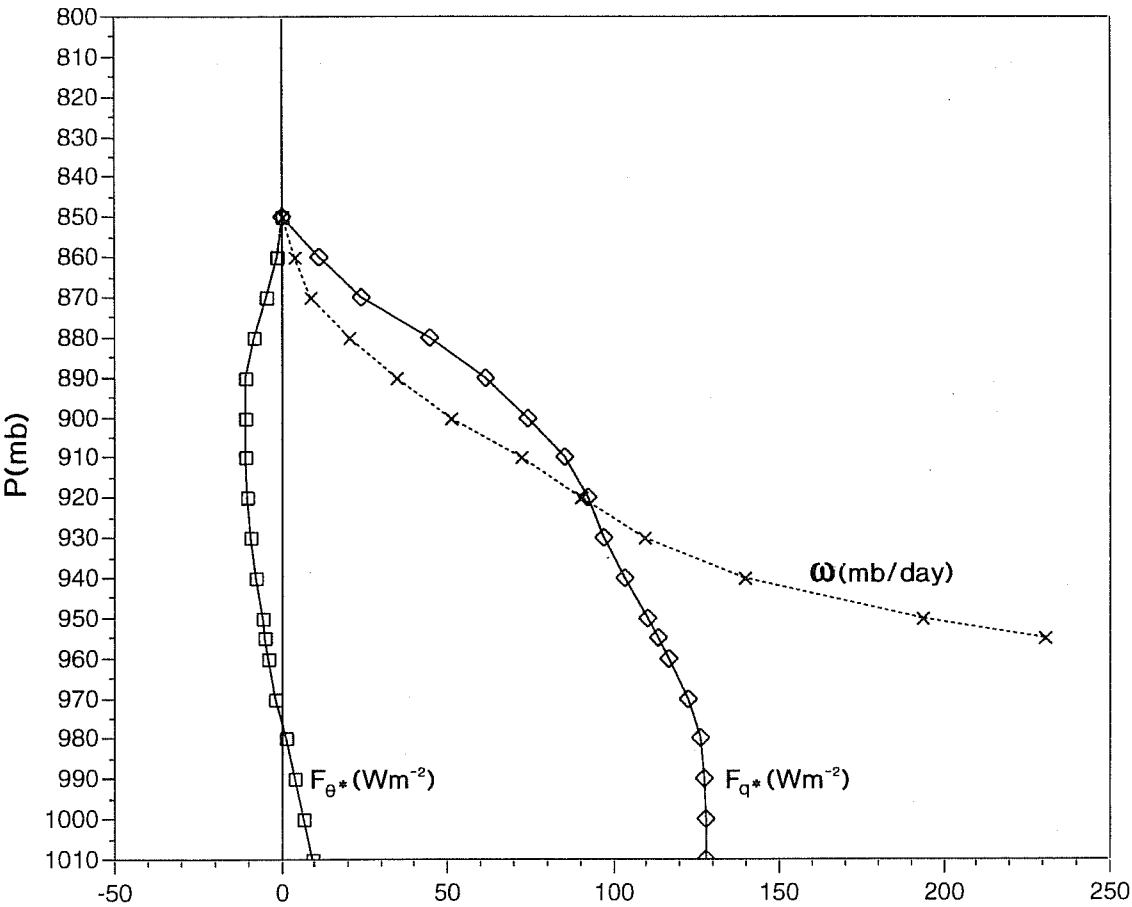

Fig. 4 Convective fluxes (solid) derived from profiles in Fig 2, and assumed subsidence and radiative cooling in CBL. Convective mass flux (dashed) derived from moisture flux.

and $\omega_o/g = \bar{\rho} C_T V_o$ (density, bulk transfer coefficient and wind-speed). The same velocity scale (ω_o/g) is then used to represent the other fluxes: for example, the length of the radiative cooling vector $(\Delta\theta_N)$ is

$$C_p(\omega_o/g)\Delta\theta_N = \Delta R_N \qquad (2)$$

where ΔR_N is the net radiative flux difference across the subcloud layer. Typically

$\Delta R_N \sim 15\ Wm^{-2}$, $\omega_o \sim 80\ mb/day$

giving $\Delta\theta_N \sim 1.6\,K$. In Fig 3 the cloud-base vector and subsidence vectors are schematically drawn from the budget estimates made in section 3.

The tradewind cloud layer is not well-mixed. The air transported through cloud-base with the properties of air from say 1000 mb is distributed through the cloud-layer with a cloud mass flux that decreases with height (*Betts*, 1975, 1985b). *Betts* (1985b) showed how the decrease and rotation of the cloud thermodynamic flux vector with height can balance the net radiative cooling, layer by layer, and produce the smooth change in structure that we also see here. The cloud layer is not well mixed, but if we integrate over it (from 850-960 mb), we can schematically show the equilibrium of the whole layer as the vector balance shown. The heavy dot at $(\theta,q) = (300.18K, 11.4gkg^{-1})$ is the mean SP of the cloud layer. Its equilibrium is a balance of the cloud-base flux (direction reversed), the subsidence of warm, dry air into the layer (this is mixed downwards by the clouds so that the trade inversion is maintained with a top at 850 mb, as the air at this level subsides in balance with the radiative cooling), and the radiative cooling ($\approx$30 Wm^{-2}) of the cloud layer itself.

The subcloud layer is nearly well mixed because its internal mixing timescale (τ_{BI}) is much shorter than the surface flux timescale of

$$\tau_o \sim \Delta p_s/\omega_o \sim 50/80 \sim 0.63\ days.$$

We can estimate τ_{BI} roughly from the surface convective velocity-scale $\omega_{o*} = g\left(\frac{\bar{\rho} F_{o\theta}\Delta p_B}{C_p\theta}\right)^{1/3} \sim 5.5\ Pa\,s^{-1} \sim 5000\ mb\,day^{-1}$ where $F_{o\theta}$ is the surface heat flux $(\sim 10\ Wm^{-2})$, Δp_B the pressure thickness of the subcloud layer of 50 mb. In the dry convective layer, regions of ascent and descent are roughly equal, so we can estimate the internal circulation time-scale as the subcloud layer $\tau_{BI} = 50/\omega_{*o} = 0.01\ days$ (or 15 mins).

Since $\tau_{BI} << \tau_o$, the subcloud layer is nearly well mixed.

However for the cloud layer, the internal timescale is much longer. An estimate can be made from the convective mass flux. Near cloud-base this may be as high as 300 mb/day, falling to below 50 mb/day near the inversion-base (see section 3). Correspondingly the internal timescale for mixing in a 100 mb thick cloud layer would rise with height from $\approx$ 0.33 days in the lower cloud layer to over one day in the inversion layer (see section 3). Qualitatively the wider spread of SP in Fig 2 in the inversion layer reflects this.

2.2 Mass flux model fit to Trade cumulus equilibrium

Fig 2 shows the equilibrium structure of a tradewind layer in the eastern equatorial Pacific. *Betts and Ridgway* (1988) showed how the surface fluxes could be retrieved using a radiation model to estimate the radiatively driven subsidence at CBL-top, and then a mixing line model to represent the internal structure of the CBL. I will reproduce a simplified version of this analysis here for illustration, and reconstruct the convective fluxes from the surface through the CBL, together with the convective mass flux distribution in the cloud layer. A mean subsidence is first assumed with a magnitude consistent with *Betts and Ridgway* (1988). This has a simple structure: the subsidence is fixed at 40 mb/day in the cloud layer ($960 < p < 850$) and decreases linearly below cloudbase to zero at the surface (1010 mb). The simplified one dimensional moisture budget equation is then solved to give the convective flux of total moisture, which balances the subsidence (using the observed mean moisture structure

$$F_{q^*}(p) = L\int_{850}^{p} \overline{\omega}(\partial\overline{q}/\partial p)\,dp/g) \qquad (3)$$

This gives a surface moisture flux of 128 Wm^{-2}, and a cloud-base flux of 117 Wm^{-2}, both realistic values. The profile is shown in Fig 4.

If we then use the subsidence and the mean $\overline{\theta}(p)$ structure, we can estimate the radiative cooling rate which will satisfy the energy balance of the cloud and subcloud layers. We find (again consistent with BR88) that this needs a mean radiative cooling of $\dot{\theta}_R$ = -2.4 K/day to give a realistic surface flux. We use this value independent of height to retrieve a convective θ^* flux from

$$F_{\theta^*}(p) = C_p\int_{850}^{p} (\overline{\omega}\,\partial\overline{\theta}/\partial p + \dot{\theta}_R)\,dp/g \qquad (4)$$

This gives a surface heat flux of 10 Wm^{-2} and a cloud-base value of -4 Wm^{-2}, and a reasonable distribution with height through the cloud layer. Fig 4 shows the vertical structure of these convective fluxes. They are very

similar to those derived from the BOMEX data by *Holland and Rasmusson* (1973), *Nitta and Esbensen* (1974) and *Betts* (1975). A bulk aerodynamic formula

$$F_{oq^*} = L(\omega_o/g)(q_s(SST) - \bar{q}(1000)) \tag{5}$$

gives a value of ω_o of 80 mb/day corresponding to a surface windspeed of 5.2 ms^{-1} with a surface transfer coefficient of 1.3 10^{-3} (realistic for this region). The same value of ω_o gives an estimate of the $F_{o\theta*}$ from the SST and air temperature of 11.5 Wm^{-2}, which is sufficiently close to our budget value assumed in (4).

A convective mass flux can also be retrieved from the moisture flux using

$$F_{q^*}(p) = \omega^*(p)(q_c - \bar{q}) \tag{6}$$

We assumed q_c constant equal to 16.54 gKg^{-1} (the value found near the base of the subcloud layer), and derived the profile of $\omega^*(p)$ also shown in Fig 4. The cloud-base value is near 300 mb day^{-1}, falling rapidly with height, as shown by earlier studies. A similar estimate can be derived from $F_{\theta*}(p)$, but the cloud-base mass flux is very sensitive to errors of $\pm$ 0.1 K in the value of θ_c chosen, since both the θ flux and $(\theta_c - \bar{\theta})$ are small near cloud-base. However, we can say that, given a plausible value of θ_c, the convective mass flux profile derived using (6) (from the moisture flux) will match the θ^* flux from (4) to < 2 Wm^{-2}.

3. IDEALIZED MIXING MODEL FOR CBL'S

In this section, I explore a very simple lagged mixing model for a CBL, simpler than the lagged convective adjustment scheme of *Betts and Miller* (1986). Most of my results are obvious, but it is easy to lose track of the obvious, as models get more complex. The convective parametrization is just

$$(\partial\bar{S}/\partial t)_{conv} = (\hat{S} - \bar{S})/\tau \tag{7}$$

that is, mixing the horizontal mean thermodynamic properties towards a vertically homogeneous state $\hat{S}$, a suitably defined mean for the layer. We define $\hat{S}$, so that $\bar{S}$ is conserved during the adjustment when integrated over the convective layer.

$$\hat{S}\int(1/\tau)dp = \int(\bar{S}/\tau)dp \tag{8}$$

This parametrization now reduces to

a) Defining the convective layer

b) Defining the timescale of mixing (which will be allowed to be a function of pressure in one case).

Starting from the eastern equatorial Pacific sounding in Fig 2, we now apply this parametrization to this initial condition for short time periods to illustrate the impact. We fix both the radiative forcing at -2.4 K/day, and the large-scale forcing (which is set equal to the initial drying and warming produced by 40 mb/day subsidence in the cloud layer. Thus this is in no sense an interactive calculation.

3.1 Redistribution by cumulus with fixed τ = 36 000 seconds

A time-step of 1000 seconds is used in these examples. The surface fluxes are first treated separately by incrementing the subcloud layer (1010-960 mb) in q by 0.10 gKg^{-1}, and θ by 0.02 K. This corresponds to latent and sensible surface fluxes of 128 Wm^{-2} and 10 Wm^{-2}, evenly distributed through the 50 mb subcloud layer. The intent is to mimic simply the impact of a dry BL scheme. The radiative and large-scale forcing are fixed. The parametrization (7) is then used from the surface to inversion top with a fixed τ = 36 000 seconds (10 hours), independent of height. This value was chosen because it reduces the subcloud layer, $\partial q/\partial t$, to near zero. Fig 5 shows the change from the initial q profile (solid) to the profile after 6000 seconds (dashed). The net effect of the cloud field is to transport moisture out of the subcloud layer, but there is also a significant upward transport of moisture in the cloud layer, which moistens the inversion layer. In a sense, the rate of cumulus mixing needed to keep the subcloud layer from moistening is too vigorous in the cloud layer. Fig 6 shows the change of the θ structure. The cooling of the inversion layer and warming of the lower cloud layer is qualitatively realistic, but the subcloud layer warms a lot, which is not realistic. What this means is that a mixing timescale in (7), which is sufficient to maintain the subcloud layer moisture balance, warms the subcloud layer too much to maintain equilibrium with the radiative cooling. The reason lies in the link between subcloud and cloud layers in Fig 2. The coupling of the cloud base fluxes is much closer to the slope of the dry virtual adiabat than the slope of the cloud layer mixing line. (7) when applied from surface to inversion top ignores this, and the cloud-base fluxes are determined by the slope of $(\hat{S}-S_B)$, where S_B is a subcloud layer mean. This slope is too large (negative), since $\hat{S}$ is dominated by the cloud layer mean. This is also understandable, because section 2 (and the papers cited there) show that the cloud layer fluxes can be represented by

$$F(p) = \omega^*(p)(S_c-\hat{S}) \qquad (9)$$

The differential of (9) is not equivalent to (7); it has two terms, which make different contributions to the heat and moisture budget at different levels in the cloud layer (*Betts*, 1975). However, we saw in Fig 4 that $\omega^*(p)$ decreases strongly with height. The next section attempts to mimic this by varying $\tau(p)$.

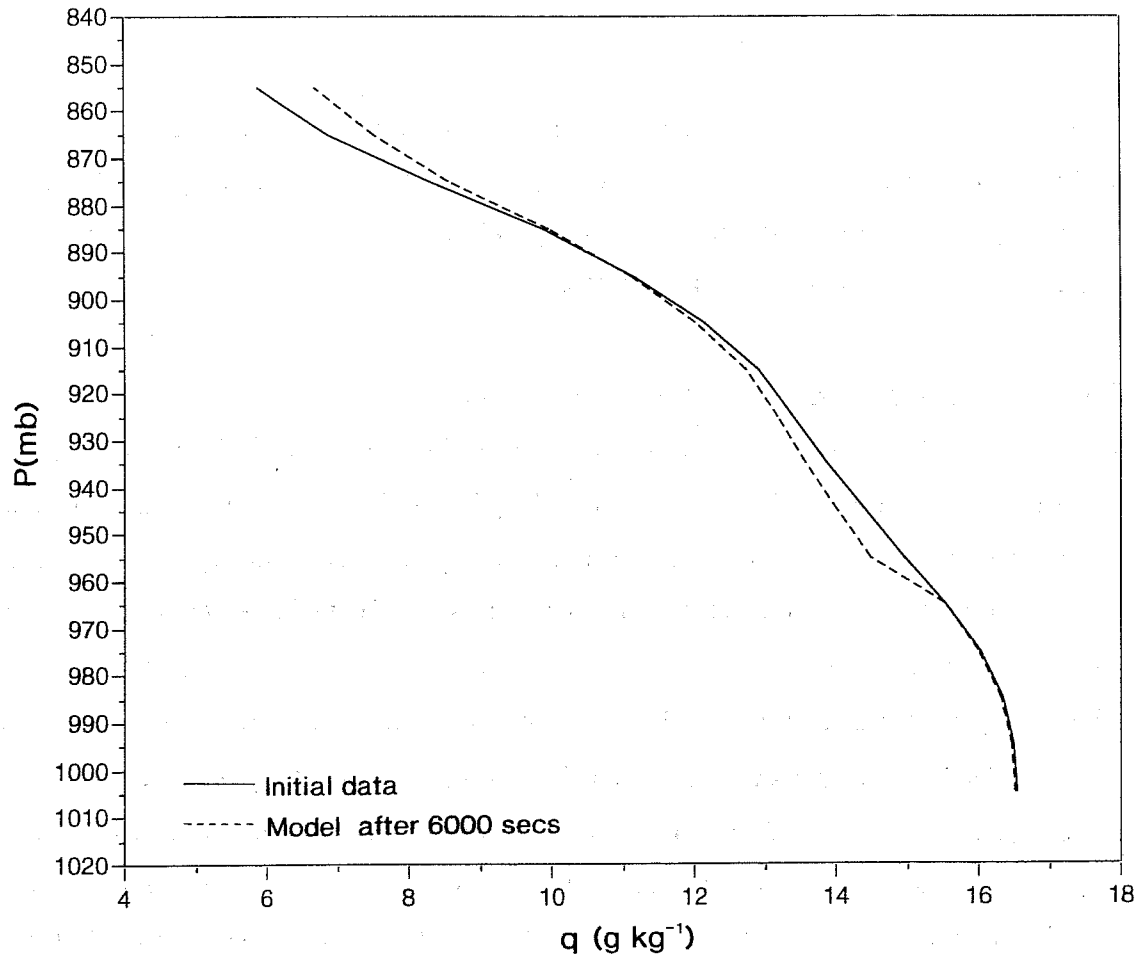

Fig. 5 Change in $q(p)$ profile after 6000 seconds with fixed τ = 36 000 seconds.

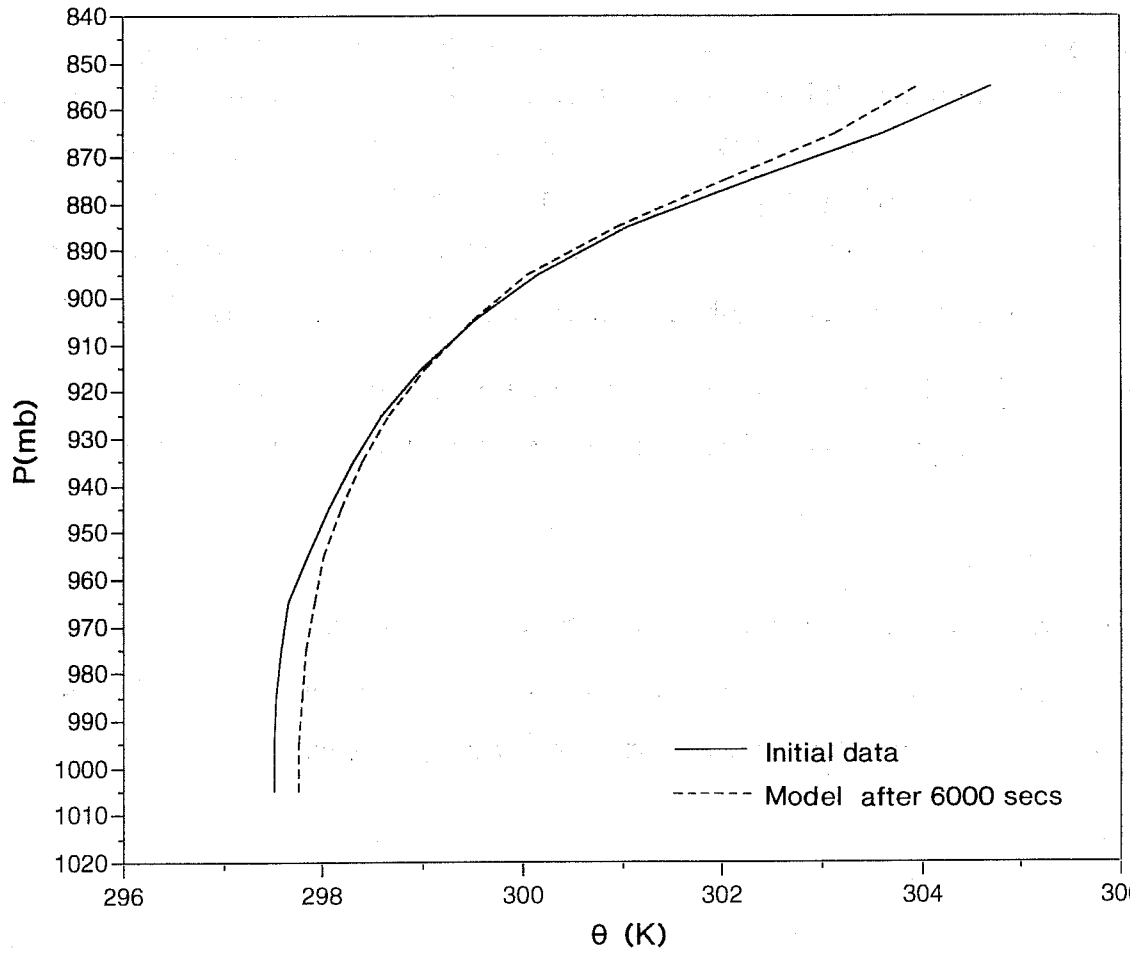

Fig. 6 As Fig. 5 for change in $\theta(p)$ profile.

3.2 Redistribution by cumulus with linear $(1/\tau)$

Suppose we qualitatively convert the mass flux in Fig 4 into a timescale, for the 110 mb thick convective layer

$$1/\tau(p) = 2\omega^*(p)/110 \qquad (10)$$

The solid line in Fig 7 shows $\tau(p)$ derived from (10). I will approximate this with the linear simplification, shown dashed, which represents an order of magnitude change in τ from 20 000 seconds near the surface to 200 000 seconds at the inversion top. Fig 8 shows the moisture change for the integration of (7) for 6000 seconds with the $\tau(p)$, and the same fixed surface and large-scale forcing. It is possible to maintain the moisture structure much more closely than with a fixed τ = 36 000 seconds. The thermal redistribution shown in Fig 9 is improved, but there is still too large a downward heat flux into the subcloud layer for the same reason as above. Fig 10 shows the rather small changes in saturation pressure departure,

$$\varrho = p^* - p \qquad (11)$$

a measure of how close each level is from saturation. The lower cloud layer remains roughly 20 mb from saturation. I show this to contrast with the next few sections.

3.3 Faster stirring (τ = 6000 seconds) in a shallower cloud layer

Suppose the mixing time constant is speeded up to a fixed 6000 seconds, from the surface to 895 mb, a little above inversion base. This could be regarded as a consequence of an artificially large parametric mixing, or rather implausibly some physical mechanism such as strong shear or enhanced cloud induced mixing (the circulations within stratocumulus have faster circulation and timescales of this order eg *Penc and Albrecht*, 1987). Fig 11 shows the subsaturation after 6000 seconds of integration with the same surface and large-scale forcing as before. The upward transport of moisture and downward transport of heat has pushed the top of this layer at 895 mb to just reach saturation, when layer cloud will form. It is clear that rapid stirring of a moist layer will produce stratocumulus in a few hours.

3.4 Fast mixing in a deeper layer, followed by uncoupling

The depth over which mixing takes place is important. If we repeat the idealized integration of the previous section with τ = 6000 seconds over a deeper layer (1010-865 mb), roughly up to the inversion top, the cloud layer does not reach saturation in the same time, because drier air is involved in the mixing at the top. Fig 12 shows the change in ϱ after 8000 seconds (dashed); the top of the layer is still 20 mb from saturation. The subcloud layer has by this time dried by 2 gKg^{-1} and warmed to 298.7 K, the sea surface temperature (not shown). This suggests one further idealized experiment. When the subcloud layer warms to the SST, we might expect the mixing in the subcloud layer to drop. So at 8000 seconds, we turn off the mixing in the

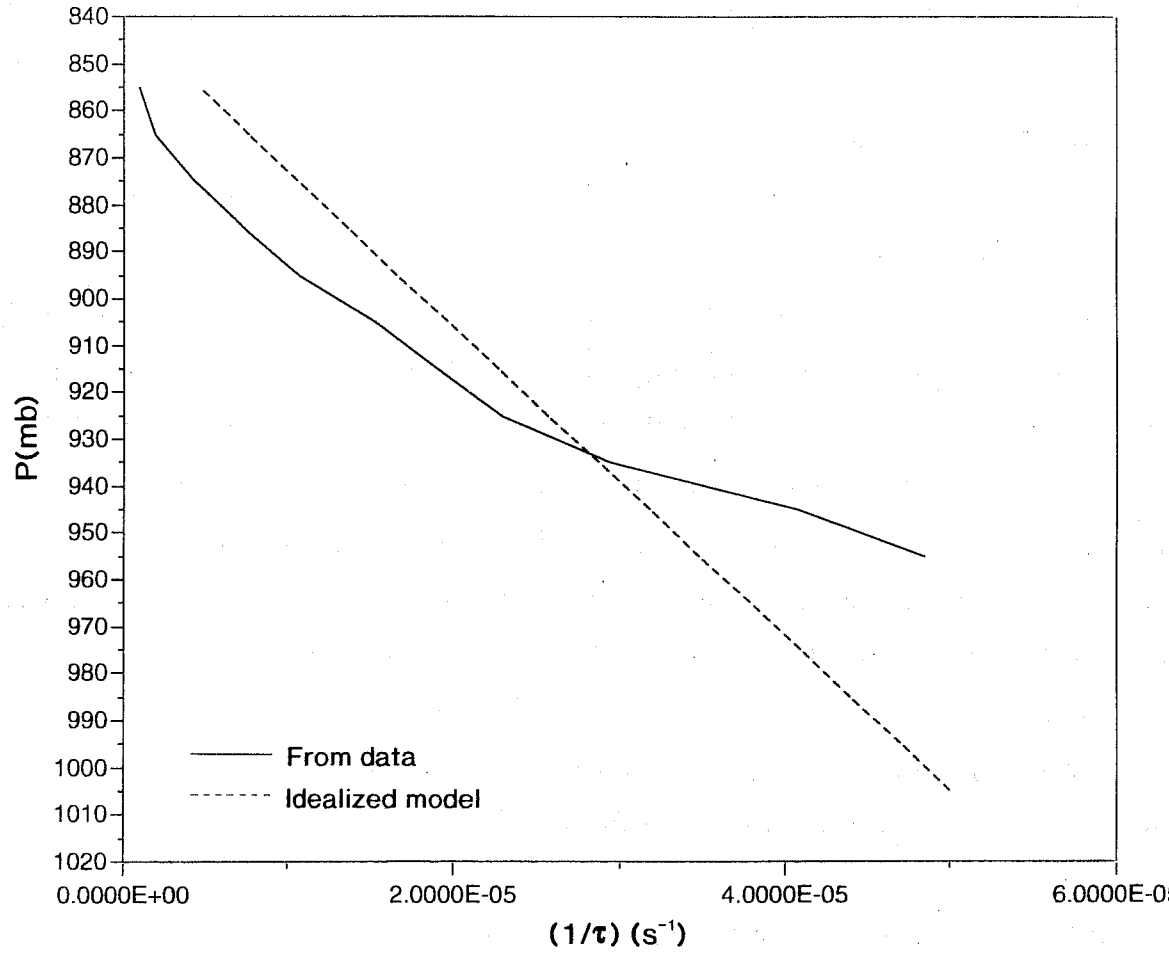

Fig. 7 Profiles of $(1/\tau)$ derived from data (solid), and used in simplified model (dashed).

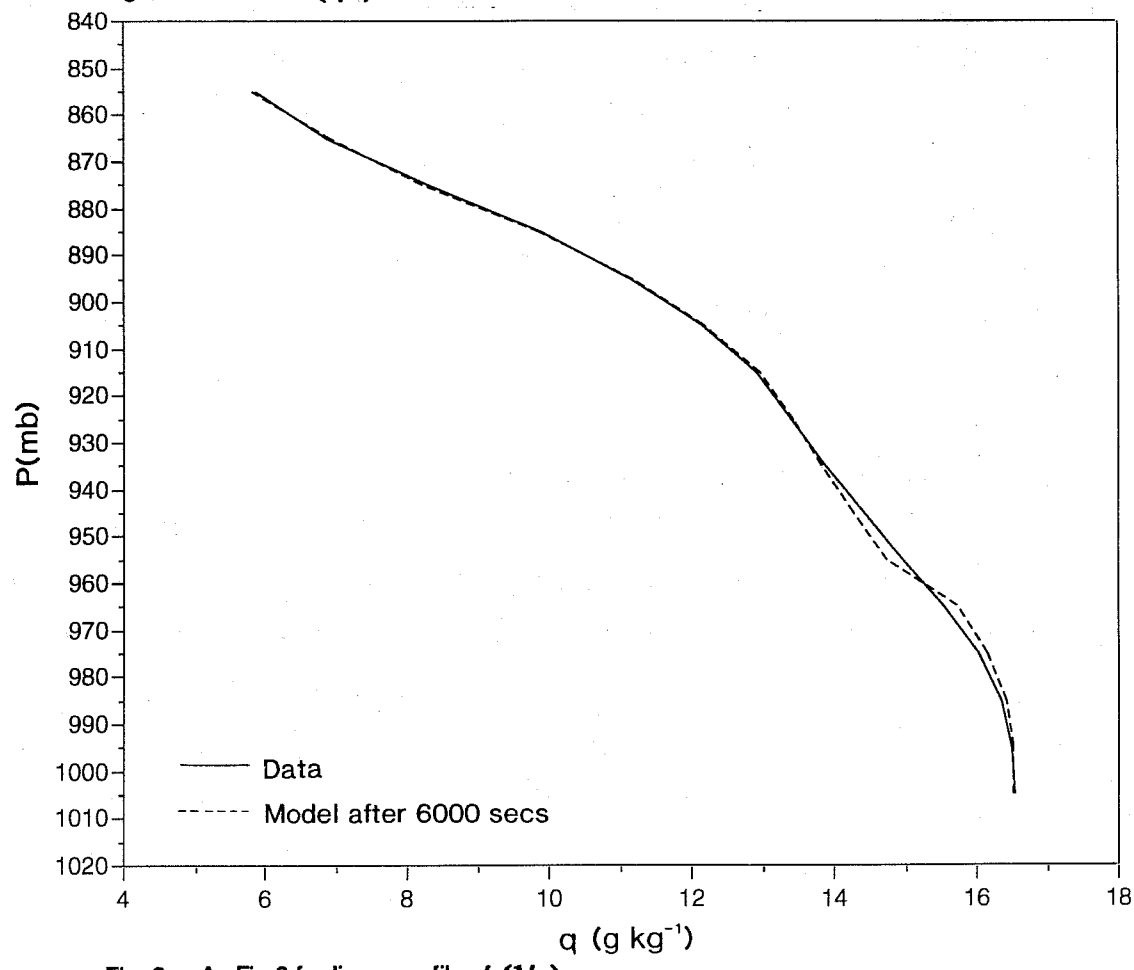

Fig. 8 As Fig 6 for linear profile of $(1/\tau)$.

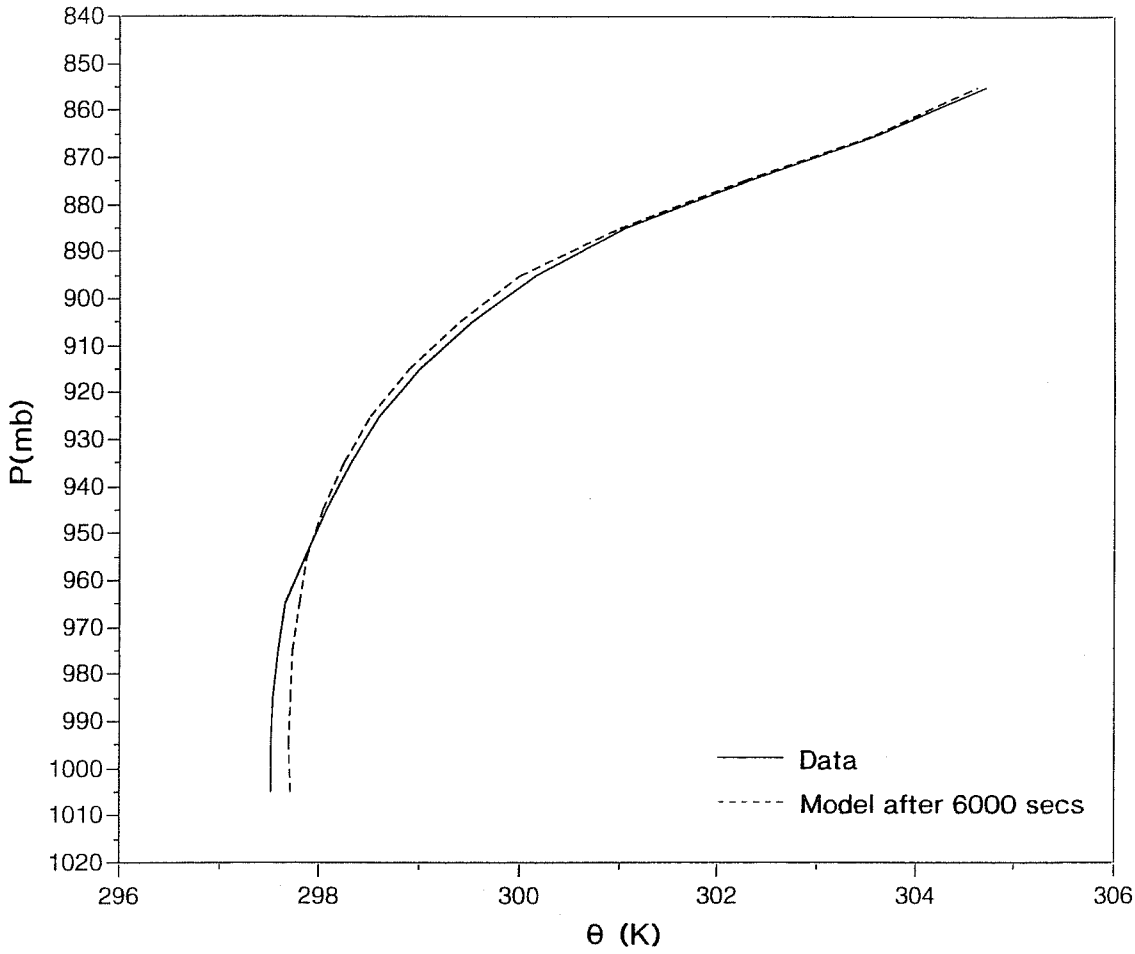

Fig. 9 As Fig 8 for θ profile change.

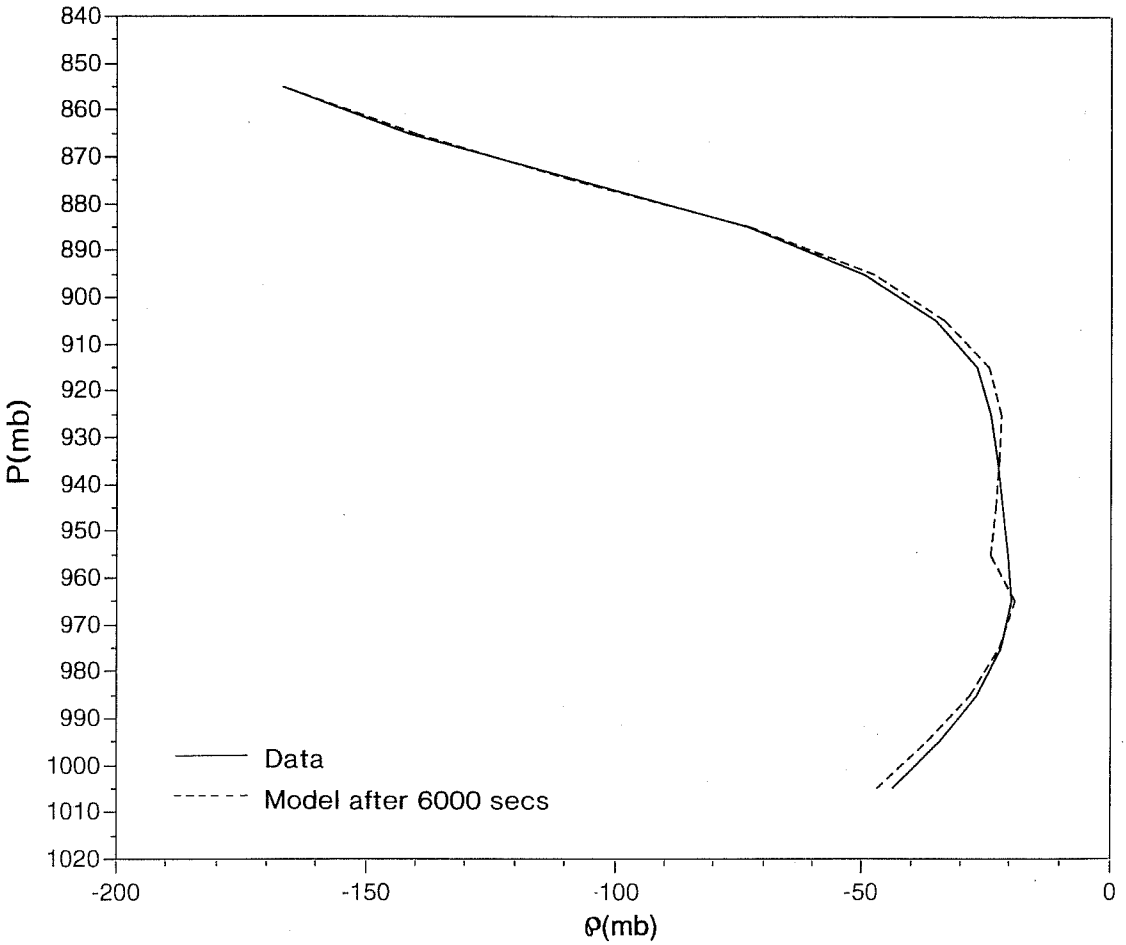

Fig. 10 As Fig 9 for change of $\rho(=p^*-p)$.

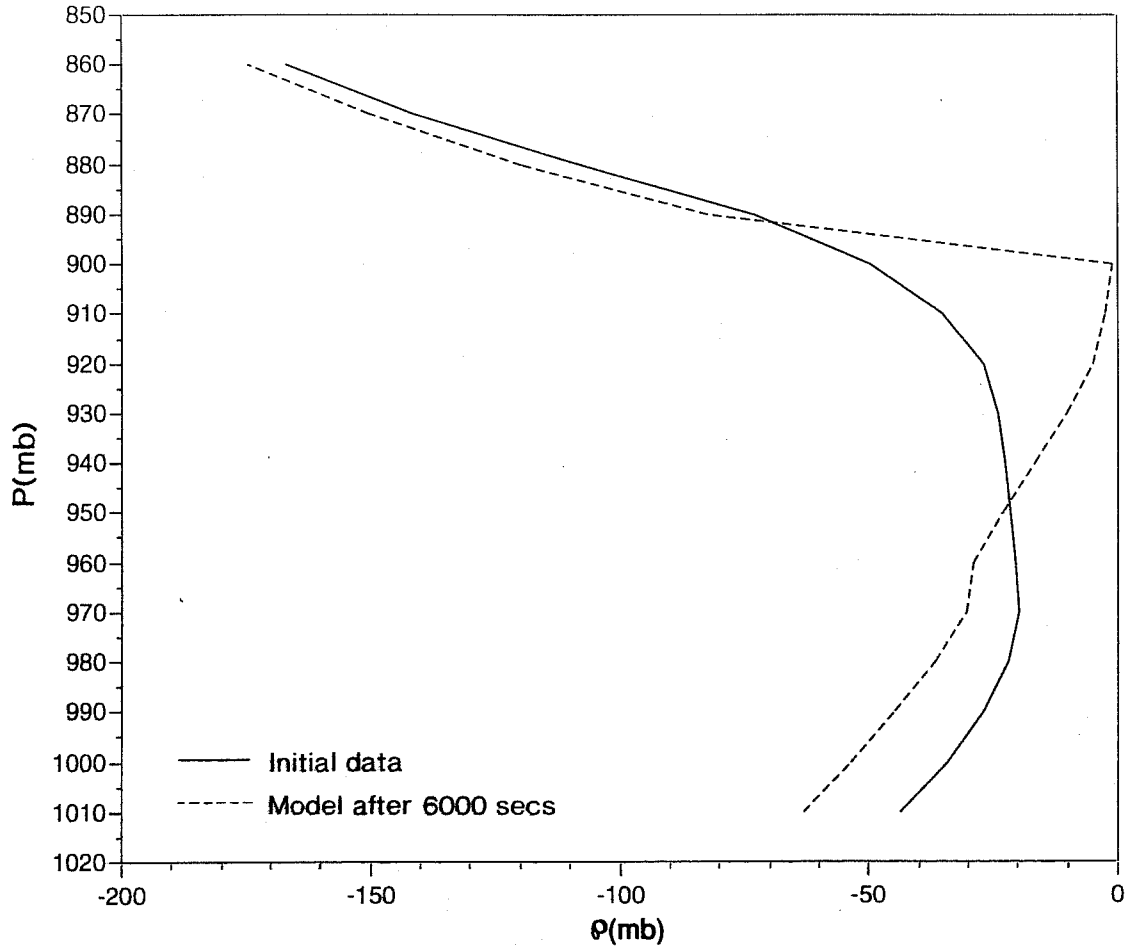

Fig. 11 Change of ρ after 6000 seconds using τ = 6000 seconds and mixing layer 895 > p > 1010 mb.

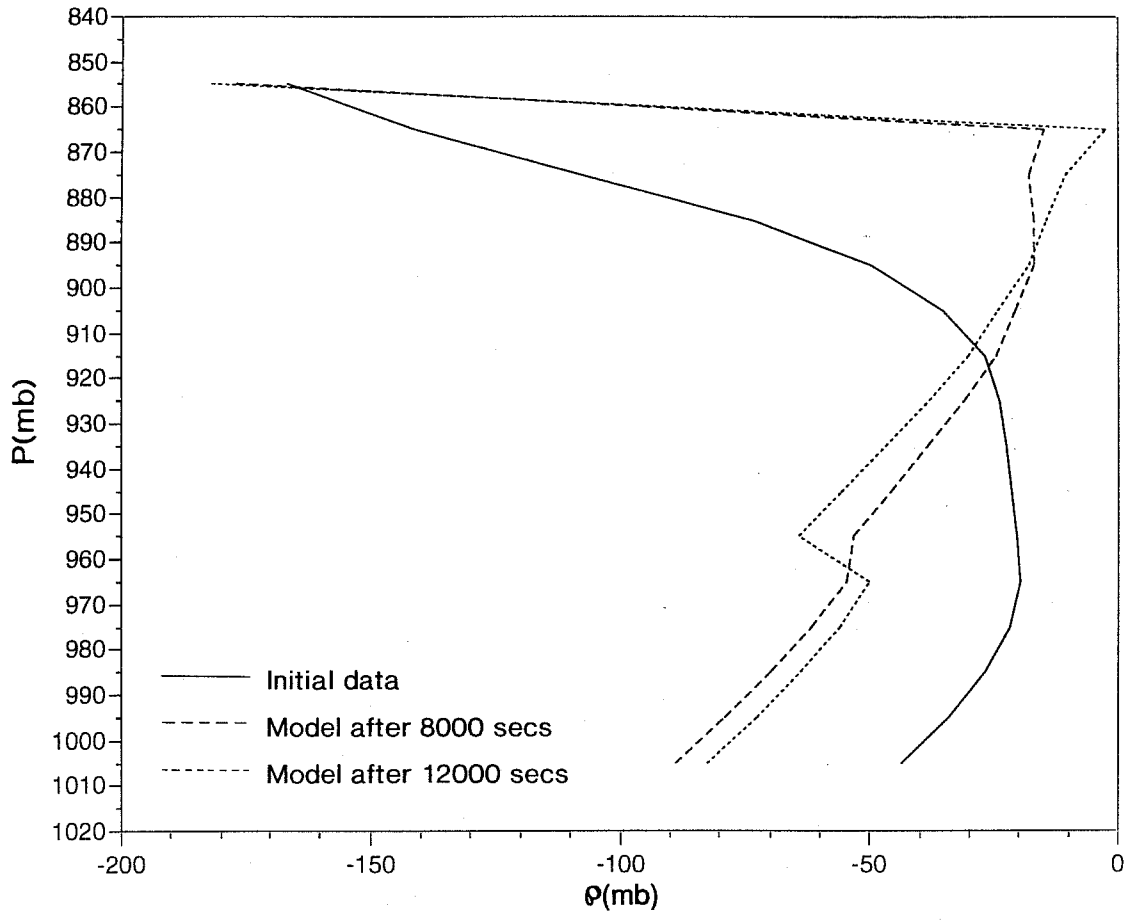

Fig. 12 As Fig 11 for deeper layer of mixing 860 > p > 1010 mb. Dashed line is at 8000 seconds; dotted line at 12 000 seconds, after uncoupling subcloud layer at 8000 seconds.

subcloud layer by setting $\tau = \infty$ for $1010 < p < 960$ mb and continue the mixing in the cloud layer ($960 < p < 860$) to 12 000 seconds. This gives the dotted profile in Fig 13. The cloud layer at this time has reached saturation at the top, and is uncoupled at cloud-base from the subcloud layer.

3.5 Discussion

These are all idealized examples, but they show that much of the range of structure that is seen in CBL's can be mimicked with a very simple parametrization, by mixing timescale varying τ and the depth of the convective layer. The problem in a parametrization is to get the convective layers and timescales right (and the interaction of different convective layers), and I have not solved these problems here. We have only a qualitative sense that for cumulus layers, τ increases with height from 2.10^4 to 2.10^5 seconds, while for stratocumulus, τ may be less $\sim 10^4$ seconds. Convective circulations are driven by warmer surfaces and radiative cooling off moist layers and cloud-tops, but simple models for circulation timescale are needed. The problem is interactive because faster stirring generates layer clouds, and layer clouds generate more stirring.

4. BOUNDARY LAYER DEEPENING OVER LAND

Defining the top of the convective layer for a parametrization scheme needs care, since it effectively controls BL-top entrainment notes. A simple mixing model for the growth of a dry mixed layer will illustrate this. The initial condition will be a mean FIFE sounding at 1700Z (approx 1100L) in July 1987 near Manhattan, Kansas. We will consider the time interval 1700-1830 Z for which we have mean sonde profiles and surface fluxes. The mean surface fluxes are (SH, LH) of (114, 388) Wm^{-2}. We use a timestep Δt of 540 seconds (0.1 of the time interval of 90 minutes between the mean sondes, for convenience), and add the surface fluxes every timestep as increments to the first layer above the surface, which is 4.7 mb thick. Suppose this first layer then has potential temperature θ_{00}, after this addition of heat. The BL is then defined as the layer for which $\theta < \theta_{00}$ (ie. θ_{00} is used to define a BL-top as the equilibrium level of parcels mixing dry adiabatically from the first layer). Parametrization (7) is then used to distribute the surface fluxes through the BL. We integrate for 10 timesteps. Figs. 13 and 14 compare the observed soundings and two model integrations using two adjustment times of 1000 and 1500 seconds (independent of height). The parametrization does a good job of generating a mixed layer, and simulating BL-top entrainment, since the equilibrium level of parcels rising from the surface involves some overshoot. However, the effective entrainment is too small for $\tau = 1000$, and too large for the $\tau = 1500$ seconds. This model is sufficiently simple that we can explore it analytically. The entrainment depends on θ_{00}. θ_{00} is determined within a few timesteps by a balance of the added surface

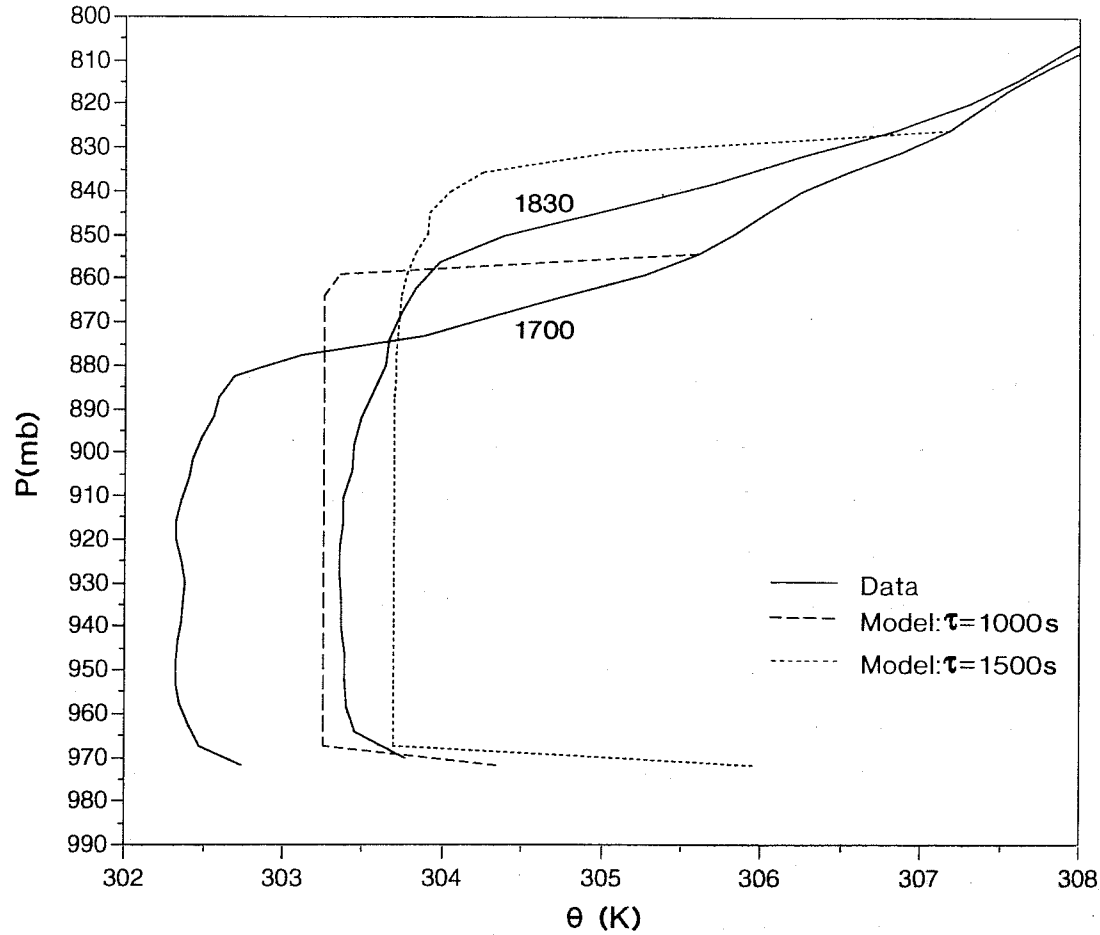

Fig. 13 Comparison of FIFE July average sonde θ profiles at 1700 and 1830Z (solid) with integration of mixing parametrization from 1700 to 1830 with adjustment time of 1000 (dashed) and 1500 seconds (dotted).

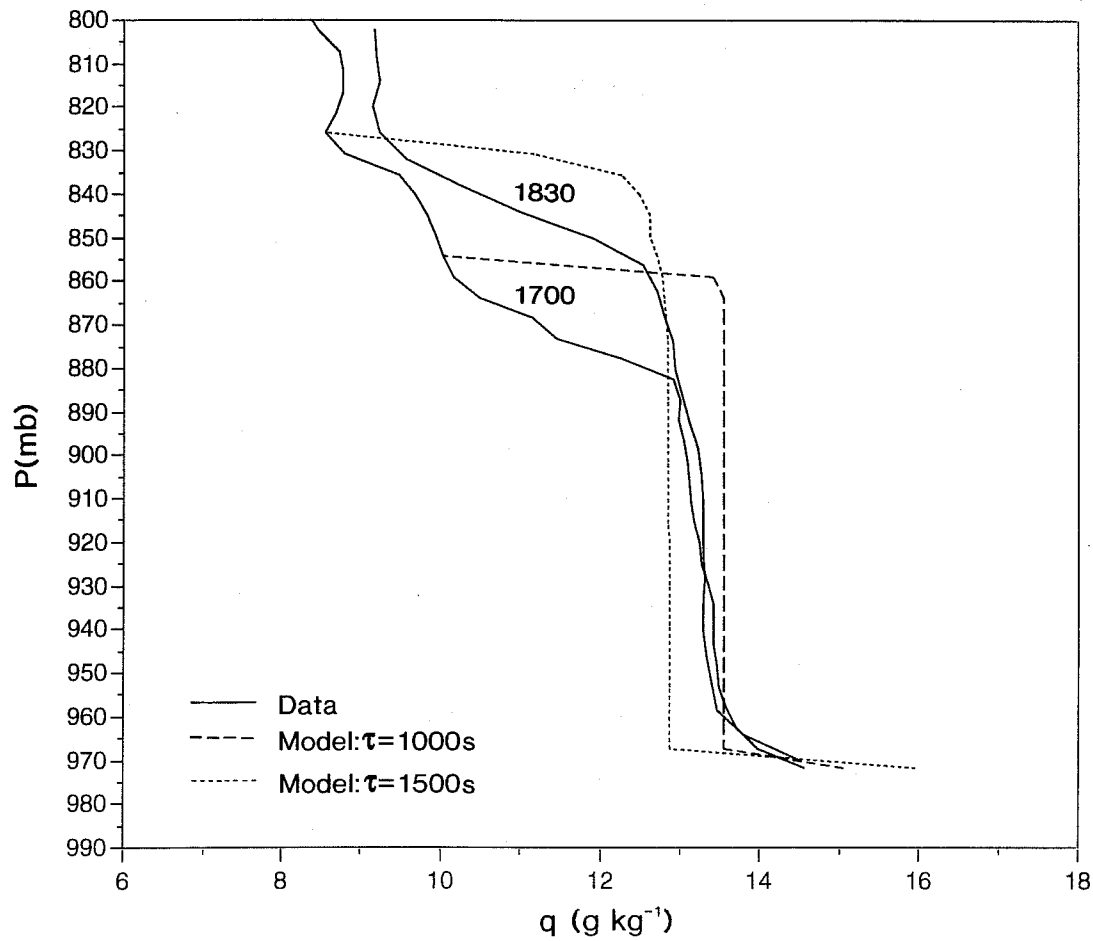

Fig. 14 As Fig 13 for *q* profiles.

energy and the lagged adjustment. This balance can be written

$$\frac{(\hat{\theta}-\theta_{00})}{\tau}\Delta t + \frac{gF_{0\theta}\Delta t}{C_p\Delta p_i} = 0 \tag{12}$$

where $F_{0\theta}$ is the surface heat flux and Δp_i the first layer thickness. The timestep Δt cancels, giving the θ excess of the first layer as a lagged value related to adjustment time, surface heat flux, and layer depth

$$\Delta\theta = (\theta_{00}-\hat{\theta}) = \tau(gF_{0\theta}/C_p\Delta p_i) \tag{13}$$

For τ=1000*secs*,, (13) gives 2.1 K. The longer τ (or smaller Δp_i), the larger $\Delta\theta$, the higher the equilibrium level and correspondingly the model entrainment. It could be argued that this is an oversimplified model for the dry BL, where it is customary to solve for the surface flux and BL fluxes simultaneously. However, consider a cumulus parametrization where the dry convective BL model is first called, and then the cumulus parametrization using sub-cloud layer parameters. The interaction of different sequential components of a model's parametrization must be carefully considered to assess whether the overall physics is properly simulated. This rather than greater detail in individual sub-models needs to be a priority.

In this simple model, the entrainment rate, ω_e can be extracted explicitly. Using the mixed layer budget as

$$\frac{\partial\hat{\theta}}{\partial t} = g(F_{0\theta}-F_{I\theta})/C_p\Delta p = \frac{\partial\theta^+}{\partial t} = \Gamma^+\omega_e \tag{14}$$

and the entrainment flux as $gF_{I\theta} = \omega_e C_p\Delta\theta$, (where $\Delta\theta = \theta_{00}-\hat{\theta}$), we can extract ω_e as

$$\omega_e = \left[\frac{C_p\Gamma^+\Delta p}{gF_{0\theta}} - \frac{\tau}{\Delta p}\right]^{-1} \tag{15}$$

where Γ^+ is $(-\partial\theta/\partial p) \approx$ 5 K/100 mb above the BL, and Δp is the BL depth. The first term is the reciprocal of the BL growth by encroachment

$$\omega_{enc} = (gF_{0\theta}/C_p\Gamma^+\Delta p) \tag{16}$$

so that ω_e is determined by 2 terms

$$\omega_e = \left[\frac{1}{\omega_{enc}} - \frac{\tau}{\Delta p_i}\right]^{-1} = \omega_{enc}\left[1-\frac{\tau\omega_{enc}}{\Delta p_i}\right]^{-1} \tag{17}$$

The terms are actually related to the balance of two physical processes: how fast the surface flux warms the mixed layer, and how large a temperature excess is maintained in the near-surface superadiabatic layer by the

surface heating as heat is transferee up into the mixed layer. Our parameterization of the latter is very simple. We added all the heat to one layer, so that this term looks like an artifact of the pressure grid, but clearly one could relate Δp_i to the depth of the surface layer and τ to a convective timescale. τ could also be chosen to give the proper entrainment rate (if we knew it!). Finally we note that the ratio of the entrainment flux to the surface flux is $A_R = \dfrac{C_p \omega_e \Delta\theta}{g F_{o\theta}} = \dfrac{\omega_e \tau}{\Delta p_i} = \left[\dfrac{\Delta p_i}{\tau \omega_{enc}} - 1 \right]^{-1}$

This ratio (in terms of virtual fluxes) has often been used as a parametric closure.

5. CONCLUSIONS

This paper is rather incomplete. I wished to draw attention to the role of different timescales in BL mixing processes, and urge that attention be given to trying to determine timescales for mixing from data and models of different scales. My second point is that it may be more important to address the interaction of different components of the surface, dry BL, cloudy BL (and radiation) schemes, than to add greater detail to any one scheme. This is not an easy task. I hope to do more work on the land-surface interaction problem in the coming year.

Acknowledgements

This research has been supported by NSF under ATM90-01960 and NASA-GSFC under Contract NAS5-31738. ECMWF supported this visit.

References

Betts, A.K., 1975: Parametric Interpretation of Trade-Wind Cumulus Budget Studies. J. Atmos. Sci., 32, pp. 1934-1945.

Betts, A.K., 1982: Saturation Point Analysis of Moist Convective Overturning. J. Atmos. Sci., 39, 1484-1505.

Betts, A.K., 1985a: Mixing line analysis of clouds and cloudy boundary layers. J. Atmos. Sci., 42, 2751-2763.

Betts, A.K., 1985b: Vector representation of Trade cumulus thermodynamic fluxes. Mon. Wea. Rev., 113, 2173-2175.

Betts, A.K., 1986: A new convective adjustment scheme. Part I:Observational and theoretical basis. Quart. J. Roy. Meteor. Soc., 112, 677-692.

Betts, A.K. and M.J. Miller, 1986: A new convective adjustment scheme. Part II: Single column tests using

GATE-wave, BOMEX, ATEX, and Arctic Airmass data sets. Quart. J. Roy. Meteor. Soc., 112, 693-710.

Betts, A.K., and B.A. Albrecht, 1987: Conserved variable analysis of boundary layer thermodynamic structure over the tropical oceans. J. Atmos. Sci., 44, 83-99.

Betts, A.K. and W. Ridgway, 1988 : Coupling of the radiative, convective and surface fluxes over the equatorial Pacific. J. Atmos. Sci., 45, 522-536.

Betts, A.K., 1989: Idealized stratocumulus models and cloud layer thickness. Tellus, 41A, 246-254.

Betts, A.K., 1992: FIFE Atmospheric Boundary Layer Budget Methods. J.G.R., 97, 18523-18531.

Betts, A.K., R.L. Desjardins, and J.I. MacPherson, 1992: Budget analysis of the Boundary Layer grid flights during FIFE-1987. J.G.R., 97, 18533-18546.

Holland, J.Z., and E. Rasmusson, 1973: Measurements of the atmospheric mass energy and momentum budgets over a 500 kilometer square of tropical ocean. Mon. Wea. Rev. 101, 44-55.

Miller, M.J., A.C.M. Beljaars, and T.N. Palmer 1993: The sensitivity of the ECMWF model to the parameterization of evaporation from the tropical oceans. J. Clim., 5, 418-434.

Nitta, T. and S. Esbensen, 1974: Heat and moisture budgets using BOMEX data. Mon. Wea. Rev., 102, 17-28.

Penc, R.S. and B.A. Albrecht, 1987: Parametric representation of heat and moisture fluxes in cloud-topped layers. Boundary-Layer Meteor.,38, 225-248.